Scattering by a Narrow Gap

THOMAS B. A. SENIOR, FELLOW, IEEE, KAMAL SARABANDI, AND JOHN R. NATZKE, STUDENT MEMBER, IEEE

Abstract—**For a plane wave incident on a cavity-backed gap in a perfectly conducting plane, the coupled integral equations for the induced currents have been solved numerically and the far-field scattering computed. The results are compared with a quasi-analytic solution previously derived, and for a narrow gap the agreement is excellent for all cavity geometries and for all material fillings that have been tested.**

I. INTRODUCTION

A TOPIC OF SOME concern in radar cross section studies is the scattering from the gap or crack that may exist where two component parts of a target come together. Even if the crack is wholly or partially filled with a material, it can still provide a significant contribution to the overall scattering pattern of the target, and it is then necessary to develop methods for predicting the scattering.

One method for doing this was described recently [1]. For a plane wave of either principal polarization incident on a narrow ($kw \lesssim 1$) resistive strip insert in an otherwise perfectly conducting plane, the low frequency approximations to the integral equations for the currents induced in the strip were solved in a quasi-analytic manner, leading to expressions for the far zone scattered field that are accurate for almost any resistivity R of the insert. If, instead, the insert is characterized by a surface impedance η, the results differ only in having R replaced by $\eta/2$ and the scattered field doubled; this suggests that for a narrow gap backed by a cavity, the scattered field can be obtained by identifying η with the impedance looking into the cavity.

An alternative approach is to use the equivalence principle [2] to develop coupled integral equations for the electric and magnetic currents which exist on the walls of the cavity and in the aperture, and this is the method employed here. For an incident plane wave either H- or E-polarized, the integral equations are derived for a cavity of arbitrary shape filled with a homogeneous material. The equations are solved by the moment method, and data for a variety of simple cavities are presented. For gap widths that are electrically small, the results are compared with those obtained using the previous method. The agreement is excellent, and confirms the utility of the original method [1] as an accurate and simple design tool.

II. FORMULATION

The problem considered is the two-dimensional one shown in Fig. 1. The plane $y = 0$ is perfectly conducting apart

Manuscript received March 22, 1989; revised September 5, 1989.

The authors are with the Radiation Laboratory, Electrical Engineering and Computer Science Department, University of Michigan, Ann Arbor, MI 48109-2122.

IEEE Log Number 9035923.

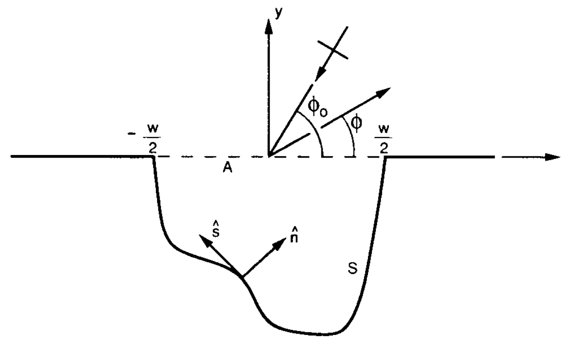

Fig. 1. Gap geometry.

from the aperture A: $-w/2 < x < w/2$, which forms the entrance to a cavity whose walls S are also perfectly conducting. The cavity is filled with a homogeneous dielectric material of permittivity $\epsilon_1 = \epsilon_r\epsilon$ and permeability $\mu_1 = \mu_r\mu$, where the quantities without subscripts refer to free space. A plane wave of either principal polarization is incident on the surface $y = 0$ from above, and we choose

$$\bar{H}^i, \bar{E}^i = \hat{z}e^{-ik(x \cos \phi_0 + y \sin \phi_0)} \tag{1}$$

for H- and E-polarizations, respectively, where k is the propagation constant in the free space region above the surface. A time factor $e^{-i\omega t}$ is assumed and suppressed.

In the far zone of the gap the scattered field can be written as

$$\bar{H}^s = \hat{z}\sqrt{\frac{2}{\pi k\rho}}\, e^{i(k\rho - \pi/4)} P_H(\phi, \phi_0)$$

for H-polarization, with a similar result for E-polarization, and the task is to determine the far-field amplitudes $P_{H,E}(\phi, \phi_0)$ with particular emphasis on the case of a narrow gap ($kw \lesssim 1$).

A. H-Polarization

We consider first the free space region $y > 0$. Using Green's theorem in conjunction with the half-space Green's function for a hard surface $y = 0$, the scattered field can be attributed to a magnetic current $\bar{J}^* = -\hat{y} \times \bar{E}$ in the aperture, and the total magnetic field is then

$$H_z(x, y) = H_z^i(x, y) + H_z^r(x, y) - \frac{kY}{2} \cdot \int_{-w/2}^{w/2} J_z^*(x') H_0^{(1)}(k\sqrt{(x - x')^2 + y^2})\, dx' \tag{2}$$

where

$$H_z^r = e^{-ik(x \cos \phi_0 - y \sin \phi_0)}$$

is the reflected plane wave and $Y(=1/Z)$ is the intrinsic admittance of free space. Hence,

$$P_H(\phi, \phi_0) = -\frac{kY}{2} \int_{-w/2}^{w/2} J_z^*(x') e^{-ikx' \cos \phi} \, dx' \quad (3)$$

and in the aperture

$$H_z(x, 0) = 2e^{-ikx \cos \phi_0} - \frac{kY}{2} \cdot \int_{-w/2}^{w/2} J_z^*(x') H_0^{(1)}(k|x - x'|) \, dx'. \quad (4)$$

We now turn to the region $y < 0$ occupied by the cavity. In accordance with the equivalence principle [2] it is assumed that the gap is closed with a perfect conductor, and that a magnetic current $-\bar{J}^*$ is placed just below, thereby ensuring the continuity of the tangential electric field in the open gap. The magnetic Hertz vector is therefore

$$\bar{\Pi}^*(x, y) = \frac{Y}{4k\mu_r} \int_{-w/2}^{w/2} \bar{J}^*(x') H_0^{(1)}(k_1 \sqrt{(x - x')^2 + y^2}) \, dx' \quad (5)$$

where $\bar{J}^* = \hat{z} J_z^*$, and $k_1 = k\sqrt{\epsilon_r \mu_r}$ is the propagation constant. The electric current $\bar{J} = \hat{n} \times \bar{H}$ on the cavity walls S and in the (closed) aperture A also implies an electric Hertz vector

$$\bar{\Pi}(x, y) = -\frac{Z}{4k\epsilon_r} \cdot \int_{S+A} \bar{J}(s') H_0^{(1)}(k_1 \sqrt{(x - x')^2 + (y - y')^2}) \, ds', \quad (6)$$

where the tangential unit vector $\hat{s}$ is such that $\hat{n}, \hat{s}, \hat{z}$ form a right-handed system with $\hat{n}$ directed into the cavity. Clearly, $\bar{J}(s) = \hat{s} J_s(s)$, and in the aperture $\hat{s} = \hat{x}$. The total magnetic field is given by (5) and (6):

$$\bar{H}(x, y) = \hat{z} \frac{kY}{4} \epsilon_r \cdot \int_{-w/2}^{w/2} J_z^*(x') H_0^{(1)}(k_1 \sqrt{(x - x')^2 + y^2}) \, dx' + \frac{i}{4} \cdot \int_{S+A} \nabla H_0^{(1)}(k_1 \sqrt{(x - x')^2 + (y - y')^2}) \times \bar{J}(s') \, ds', \quad (7)$$

and by allowing the observation point to approach the boundary of the closed cavity, we can construct an integral equation for the currents, namely

$$J_s(s) = \frac{kY}{2} \epsilon_r \cdot \int_{-w/2}^{w/2} J_z^*(x') H_0^{(1)}(k_1 \sqrt{(x - x')^2 + y^2}) \, dx' + \frac{ik_1}{2} \cdot \int_{S+A} J_s(s') \sin \gamma' H_1^{(1)}(k_1 \sqrt{(x - x')^2 + (y - y')^2}) \, ds' \quad (8)$$

where

$$\sin \gamma' = \hat{z} \cdot \frac{(x - x')\hat{x} + (y - y')\hat{y}}{\sqrt{(x - x')^2 + (y - y')^2}} \times \hat{s}', \quad (9)$$

valid at all points of S and A.

The only remaining task is to enforce the continuity of H_z through the aperture. For an observation point in the aperture, (7) becomes

$$H_z(x, 0) = \frac{kY}{4} \epsilon_r \int_{-w/2}^{w/2} J_z^*(x') H_0^{(1)}(k_1 |x - x'|) \, dx' + \frac{1}{2} J_s(s) + \frac{ik_1}{4} \cdot \int_{S+A} J_s(s') \sin \gamma' H_1^{(1)}(k_1 \sqrt{(x - x')^2 + y^2}) \, ds', \quad (10)$$

and when this is equated to the expression (4) for $H_z(x, 0)$ on the outside of the gap, we obtain

$$2e^{-ikx \cos \phi_0} = \frac{kY}{2} \int_{-w/2}^{w/2} J_z^*(x') H_0^{(1)}(k|x - x'|) \, dx' + \frac{kY}{4} \epsilon_r \int_{-w/2}^{w/2} J_z'(x') H_0^{(1)}(k_1 |x - x'|) \, dx' + \frac{1}{2} J_s(x) + \frac{ik_1}{4} \int_{S+A} J_s(s') \sin \gamma' \cdot H_1^{(1)}(k_1 \sqrt{(x - x')^2 + y^2}) \, ds' \quad (11)$$

valid for $-w/2 < x < w/2$. Since (8) is also valid in A, it can be used to simplify (11) by eliminating two of the integrals. The result is

$$J_s(x) = 2e^{-ikx \cos \phi_0} - \frac{kY}{2} \cdot \int_{-w/2}^{w/2} J_z^*(x') H_0^{(1)}(k|x - x'|) \, dx' \quad (12)$$

valid for x in A, and (8) and (12) constitute a pair of coupled integral equations for $J_z^*(x)$ and $J_s(s)$. These are the equations that will be used, and we note the similarity of (12) and (4).

When the maximum dimension of the cavity is electrically small, the Hankel function $H_0^{(1)}$ can be replaced by its logarithmic approximation, and though this does not significantly simplify the numerical solution of (8) and (12), the fact that $e^{-ikx \cos \phi_0}$ can also be replaced by unity shows that $J_z^*(x)$ and $J_s(s)$ are aspect independent. The same approximation to (3) then leads to a far-field amplitude which is independent of ϕ and ϕ_0, and this is a feature of the low frequency situation.

B. E-Polarization

The procedure is similar to that given above. For the region $y > 0$ Green's theorem in conjunction with the Green's function for a soft surface $y = 0$ gives

$$E_z = E_z^i + E_z^r + \frac{i}{2} \frac{\partial}{\partial y} \cdot \int_{-w/2}^{w/2} J_x^*(x') H_0^{(1)}(k \sqrt{(x - x')^2 + y^2}) \, dx'$$

where $\bar{J}^* = \hat{x} J_x^*$ is the assumed magnetic current in the gap and

$$E_z^r = -e^{-ik(x \cos \phi_0 - y \sin \phi_0)}$$

is the reflected plane wave. Hence

$$P_E(\phi, \phi_0) = -\frac{k}{2} \sin \phi \int_{-w/2}^{w/2} J_x^*(x') e^{-ikx' \cos \phi} \, dx', \quad (13)$$

and since $H_x = -(iY/k)(\partial E_z / \partial y)$, the tangential component of the magnetic field in the aperture is

$$H_x(x, 0) = -2Y \sin \phi_0 e^{-ikx \cos \phi_0} - \frac{kY}{2} \left(1 + \frac{1}{k^2} \frac{\partial^2}{\partial x^2}\right) \cdot \int_{-w/2}^{w/2} J_x^*(x') H_0^{(1)}(k|x - x'|) \, dx'. \quad (14)$$

In the region $y < 0$ occupied by the cavity, the field can be attributed to the magnetic Hertz vector (5) with $\bar{J}^* = \hat{x} J_x$ and the electric Hertz vector (6) with $\bar{J}^* = \hat{z} J_z$. The magnetic field is therefore

$$\bar{H}(x, y) = \nabla \times \nabla \times \frac{Y}{4k\mu_r} \cdot \int_{-w/2}^{w/2} \bar{J}^*(x') H_0^{(1)}(k_1 \sqrt{(x - x')^2 + y^2}) \, dx' + \frac{i}{4} \int_{S+A} \nabla H_0^{(1)}(k_1 \sqrt{(x - x')^2 + (y - y')^2}) \times \bar{J}(s') \, ds',$$

and by allowing the observation point to approach the boundary of the closed cavity, we obtain the integral equation

$$J_z(s) = \frac{Y}{2k\mu_r} (\hat{n} \cdot \nabla) \frac{\partial}{\partial y} \cdot \int_{-w/2}^{w/2} J_x^*(x') H_0^{(1)}(k_1 \sqrt{(x - x')^2 + y^2}) \, dx' + \frac{ik_1}{2} \int_{S+A} J_z(s') \sin \gamma \cdot H_1^{(1)}(k_1 \sqrt{(x - x')^2 + (y - y')^2}) \, ds' \quad (15)$$

where

$$\sin \gamma = \hat{z} \cdot \frac{(x - x')\hat{x} + (y - y')\hat{y}}{\sqrt{(x - x')^2 + (y - y')^2}} \times \hat{s} \quad (16)$$

valid at all points of S and A.

When the observation point is in the aperture,

$$H_x(x, 0) = \frac{kY}{4} \epsilon_r \left(1 + \frac{1}{k_1^2} \frac{\partial^2}{\partial x^2}\right) \cdot \int_{-w/2}^{w/2} J_x^*(x') H_0^{(1)}(k_1|x - x'|) \, dx' + \frac{1}{2} J_z(x) + \frac{ik_1}{4} \cdot \int_{S+A} J_z(s') \sin \gamma H_1^{(1)}(k_1 \sqrt{(x - x')^2 + y^2}) \, ds'.$$

On equating this to the expression (14) for the magnetic field on the outside of the gap, and using (15) to simplify, the result is

$$J_z(x) = -2Y \sin \phi_0 e^{-ikx \cos \phi_0} - \frac{kY}{2} \left(1 + \frac{1}{k^2} \frac{\partial^2}{\partial x^2}\right) \cdot \int_{-w/2}^{w/2} J_x^*(x') H_0^{(1)}(k|x - x'|) \, dx' \quad (17)$$

for x in A in accordance with (14), and (15) and (17) constitute a pair of coupled integral equations for $J_x^*(x)$ and $J_z(s)$.

There is a third integral equation that can be developed and this has some advantages for numerical purposes. In the region $y < 0$ the electric field produced by the electric and magnetic Hertz vectors is

$$\bar{E}(x, y) = -\frac{kZ\mu_r}{4} \cdot \int_{S+A} J_z(s') H_0^{(1)}(k_1 \sqrt{(x - x')^2 + (y - y')^2}) \, ds' \, \hat{z} - \frac{i}{4} \frac{\partial}{\partial y} \int_{-w/2}^{w/2} J_x^*(x') H_0^{(1)}(k_1 \sqrt{(x - x')^2 + y^2}) \, dx' \, \hat{z},$$

and when the boundary condition on the perfectly conducting surface is applied, we find

$$J_x^*(x) = \frac{i}{2} \int_{-w/2}^{w/2} J_x^*(x') \frac{\partial}{\partial y} H_0^{(1)}(k_1 \sqrt{(x - x')^2 + y^2}) \, dx' + \frac{kZ\mu_r}{2} \int_{S+A} J_z(s') H_0^{(1)}(k_1 \sqrt{(x - x')^2 + (y - y')^2}) \, ds' \quad (18)$$

valid on $S + A$. Of course, $J_x^*(x)$ is nonzero only in A, and (17) and (18) are the pair of integral equations used to compute $J_x^*(x)$ and $J_z(s)$.

III. Quasi-Analytical Solution

An alternative approach was proposed by Senior and Volakis [1]. In effect, the problem which they considered is a uniform impedance insert in an otherwise perfectly conducting plane. If η is the surface impedance, the integral equations for H- and E-polarizations are identical to (4) and (14) respectively, with

$$H_z(x, 0) = \frac{1}{\eta} J_z^*(x), \quad H_x(x, 0) = -\frac{1}{\eta} J_x^*(x) \quad (19)$$

at the insert. At low frequencies for which $kw \ll 1$ the integral equations can be simplified, and for H-polarization it is found that

$$\frac{1}{\pi} \int_{-1}^{1} J_2(\zeta') \ln |\zeta' - \zeta| \, d\zeta' = 1 + aJ_2(\zeta) \quad (20)$$

for $-1 < \zeta < 1$ with

$$a = \frac{2i}{kw}\frac{Z}{\eta}. \tag{21}$$

$J_2(\zeta)$ is a modified current in terms of which

$$P_H(\phi, \phi_0) = i\pi\left\{A + \frac{1}{K_H(a)}\right\}^{-1} \tag{22}$$

with

$$K_H(a) = \frac{1}{\pi}\int_{-1}^{1} J_2(\zeta)\,d\zeta \tag{23}$$

and

$$A = \ln\frac{kw}{4} + \gamma - i\frac{\pi}{2}$$

where $\gamma = 0.5772157\cdots$ is Euler's constant. We observe that $P_H(\phi, \phi_0)$ is independent of ϕ and ϕ_0, and since $K_H(a)$ is real if a is

$$|P_H(\phi, \phi_0)| \leq 2 \tag{24}$$

for real a.

Similarly, for E-polarization the low frequency approximation to the integral equation is

$$\frac{\partial^2}{\partial\zeta^2}\frac{1}{\pi}\int_{-1}^{1} J_3(\zeta')\ln|\zeta' - \zeta|\,d\zeta' = 1 - bJ_3(\zeta) \tag{25}$$

for $-1 < \zeta < 1$ with

$$b = -\frac{ikw}{2}\frac{Z}{\eta} \tag{26}$$

where the modified current $J_3(\zeta)$ is such that $J_3(\pm 1) = 0$. In terms of $J_3(\zeta)$

$$P_E(\phi, \phi_0) = -\frac{i\pi}{4}(kw)^2 \sin\phi \sin\phi_0 K_E(b) \tag{27}$$

with

$$K_E(b) = \frac{1}{\pi}\int_{-1}^{1} J_3(\zeta)\,d\zeta, \tag{28}$$

and the angle dependence is explicit in the expression for $P_E(\phi, \phi_0)$.

Computer programs were written to solve (20) and (25) by the moment method and, hence, compute $K_H(a)$ and $K_E(b)$ for all complex a and b. From an examination of the results it was found that $K_H(a)$ can be approximated as

$$K_H(a) = -\frac{(a+0.15)(a+0.29)}{\left(\frac{\pi a}{2} + \ln 2\right)(a+0.15)(a+0.29) + 0.10a(a+0.20)} \tag{29}$$

for all a apart from those in the immediate vicinity of the portion $-1.1 \leq a \leq 0.3$ of the real axis in the complex a plane. In this region an empirical expression for $K_H(a)$ is

$$K_H(a) = -\frac{1}{\frac{\pi a}{2} + \ln 2 + 0.1} \tag{30}$$

and since, for other a, (30) differs from (29) by no more than 3%, it is sufficient to use (30) for all a. Similarly, for E-polarization the approximation is

$$K_E(b) = \frac{0.62}{b+1.15}\,\frac{(b+4.08)(b+7.26)(b+10.37)(b+13.43)(b+16.46)}{(b+4.27)(b+7.37)(b+10.45)(b+13.49)(b+16.50)}, \tag{31}$$

valid for all b not in the immediate vicinity of the negative real axis. For positive real b, $K_E(b) \leq 1/2$ and hence

$$|P_E(\phi, \phi_0)| \leq \frac{\pi}{8}(kw)^2 \sin\phi \sin\phi_0. \tag{32}$$

In their regions of validity, the estimated accuracy of (29)–(31) is about three percent.

To use these results to predict the scattering from a narrow gap, it was proposed that η be identified with the impedance looking into the gap, with η calculated using a simple transmission line (or other) model that takes into account the geometry and material filling of the gap. To show how this is done, consider a crack such as those illustrated in Fig. 2. For H-polarization the cavity supports a variety of transverse electric modes, but since the width w is small, the only mode which is not evanescent is the transverse electromagnetic mode, and this is the main contributor to the field in the gap. Under the assumption that this is the only mode that must be considered, the effective surface impedance η can be deduced from the input impedance Z_{1n} of a parallel plate transmission line. The voltage across the gap is

$$V = \int_{-w/2}^{w/2} E_x(x)\,dx \approx wE_x$$

and since the current I is proportional to the tangential magnetic field,

$$\eta = \frac{E_x}{H_z} = \frac{1}{w}\frac{V}{I} = \frac{Z_{1n}}{w}. \tag{33}$$

For a parallel plate transmission line whose plate separation is w, the inductance and capacitance per unit length and width are $L = \mu_0\mu_r w$ and $C = \epsilon_0\epsilon_r/w$, respectively, and the characteristic impedance is $Z_c = Z_1 w$ with $Z_1 = Z\sqrt{\mu_r/\epsilon_r}$.

The L-shaped gap in Fig. 2(b) can be viewed as two cascaded lines. The first line has length d_1 and characteristic impedance Z_c, whereas the second (of length w_2) has characteristic impedance $Z_c' = Z_1 d_2$ and is shorted. As a load its impedance is

$$Z_L = -iZ_c' \tan k_1 w_2. \tag{34}$$

The junction of these lines can be modeled as a lumped parameter pi-network whose reactance and susceptance elements

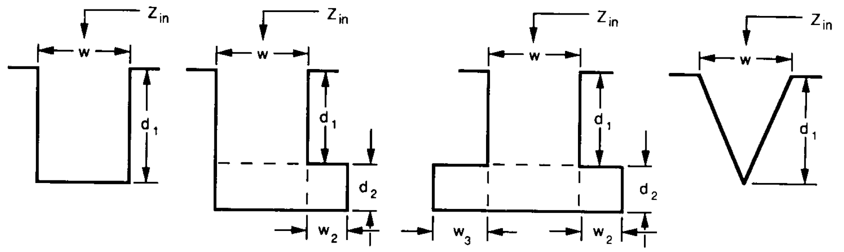

Fig. 2. Gap and cavity configurations. The cavity is filled with a homogeneous dielectric having relative permittivity ϵ_r and relative permeability μ_r.

are [3]

$$X = k_1 Z_1 w d_2$$

$$B_1 = \frac{k_1}{Z_1}\left(\frac{d_2}{d_2+w}\right)\left(1-\frac{2}{\pi}\ln 2\right)$$

$$B_2 = \frac{k_1}{Z_1}\left(\frac{w}{d_2+w}\right)\left(1-\frac{2}{\pi}\ln 2\right).$$

The input impedance of the first line cascaded with the pi-network and the second line is then

$$Z_{1n} = Z_c \frac{Z_L' - iZ_c \tan k_1 d_1}{Z_c - iZ_L' \tan k_1 d_1} \tag{35}$$

where

$$Z_L' = \frac{Z_L - iX(1 - iB_2 Z_L)}{(1 - B_1 X)(1 - iB_2 Z_L) - iB_1 Z_L}. \tag{36}$$

Similarly, the T-shaped gap in Fig. 2(c) can be treated as a transmission line loaded with two shorted lines in series. For the shorted lines of lengths w_2 and w_3, the load impedance is

$$Z_L'' = -iZ_c' \{\tan k_1 w_2 + \tan k_1 w_3\}. \tag{37}$$

The junction is modeled with a shunt susceptance and a series reactance in series with Z_L:

$$X_3 = k_1 Z_1 w d_2$$

$$B_3 = \frac{k_1}{Z_1}\left(\frac{d_2}{d_2+w}\right) 0.7822$$

where the constant was determined empirically, and the input impedance Z_{1n} is then given by (35) with

$$Z_L' = \frac{Z_L'' - iX_3}{1 - iB_3(Z_L'' - iX_3)}. \tag{38}$$

The rectangular gap is the special case $d_2 = 0$ of either of the above structures, and for this

$$Z_{1n} = -iZ_c \tan k_1 d_1. \tag{39}$$

Finally, for the V-shaped gap in Fig. 2(d), the inductance and capacitance per unit length of the line are functions of position, but when the coupled differential equations for the voltage and current are solved, we obtain

$$Z_{1n} = -iZ_c \frac{J_1(k_1 d_1)}{J_0(k_1 d_1)}. \tag{40}$$

where J_0 and J_1 are Bessel functions. For a gap of arbitrary shape, the input impedance can be determined using cascaded transmission lines of varying width, and this was verified in the case of the V-shaped gap.

For E-polarization all of the modes are evanescent, but if we again assume that the first mode dominates in the gap, simple formulas for the surface impedance can be found. In a parallel plate waveguide of width w

$$H_x = \frac{1}{ikZ\mu_r}\frac{\partial E_z}{\partial y},$$

and for the lowest order mode the propagation constant is ikp where

$$p = \left\{\left(\frac{\lambda}{2w}\right)^2 - \epsilon_r \mu_r\right\}^{1/2}. \tag{41}$$

Since E_z/H_x is independent of position, a transmission line analogy can be made. The characteristic impedance of the line is $-iZ\mu_r/p$, which is also the impedance looking into the gap, and the results previously obtained for H-polarization are now applicable if k_1 is replaced by ikp and Z_1 by $-iZ\mu_r/p$. Thus, for a rectangular gap

$$Z_{1n} = -i\frac{Z\mu_r w}{p} \tanh kpd_1, \tag{42}$$

and for a triangular gap

$$Z_{1n} = -i\frac{Z\mu_r w}{p}\frac{I_1(kpd_1)}{I_0(kpd_1)}, \tag{43}$$

where Z_{1n} and η are related via (33) and I_0 and I_1 are modified Bessel functions [4]. Formulas for L- and T-shaped cracks can be deduced in a similar manner, but since the modes are evanescent, the shape of the lower cavity has little or no effect on the impedance.

IV. Numerical Results

The integral equation pairs (8), (12) and (17), (18) for H- and E-polarizations, respectively, were programmed for solution by the moment method, using pulse basis and point matching functions. In the case of (17), the derivative was applied to the kernel, and because of the order of the resulting singularity, the contributions from two cells on either side of the self-cell were evaluated analytically, in addition to the contribution of the self-cell itself. Comparison with the results

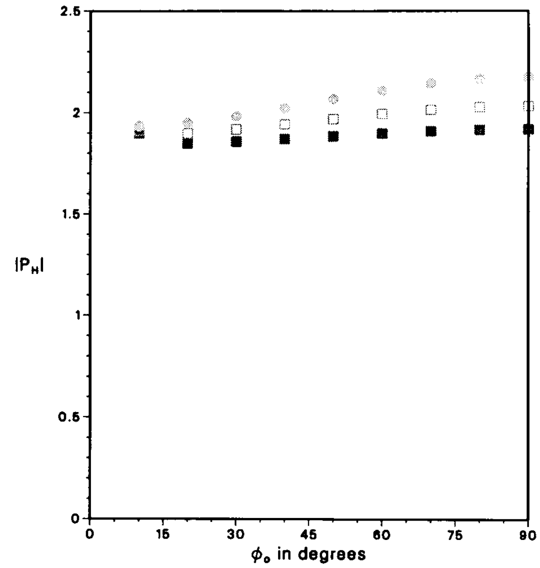

Fig. 3. Modulus of the far-field amplitude P_H with respect to aspect ϕ_0 for a rectangular gap with $\phi = \pi/2$ and $d/\lambda = 0.2$: ■ $w/\lambda = 0.15$, □ $w/\lambda = 0.2$, ● $w/\lambda = 0.25$.

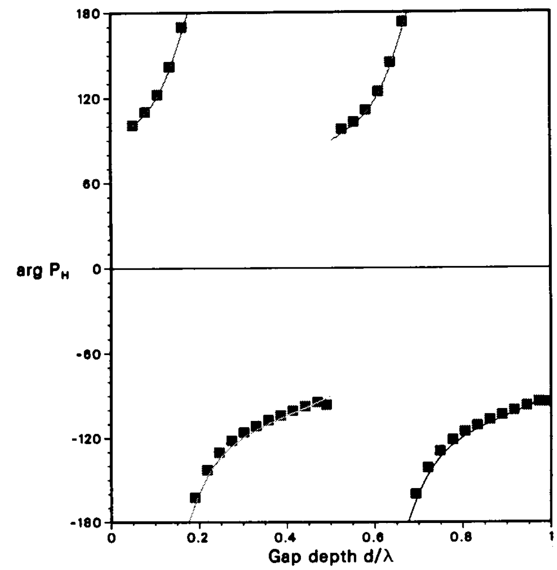

Fig. 5. Argument of the far-field amplitude P_H for a rectangular gap of varying depth $d_1 = d$ with $\phi = \phi_0 = \pi/2$ and $w/\lambda = 0.15$: ■ exact, —— analytical.

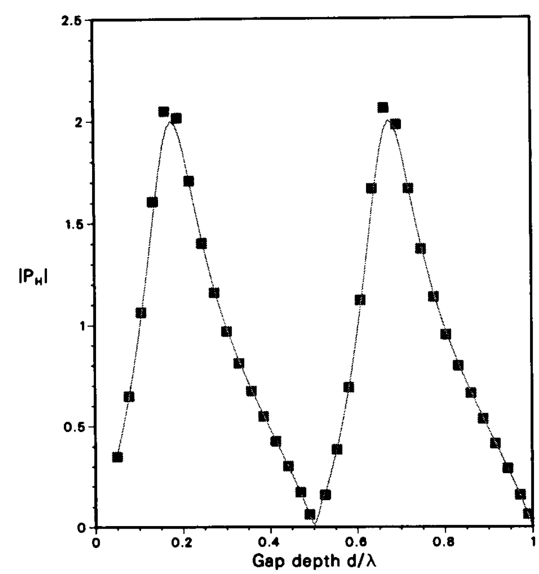

Fig. 4. Modulus of the far-field amplitude P_H for a rectangular gap of varying depth $d_1 = d$ with $\phi = \phi_0 = \pi/2$ and $w/\lambda = 0.15$: ■ exact, —— analytical.

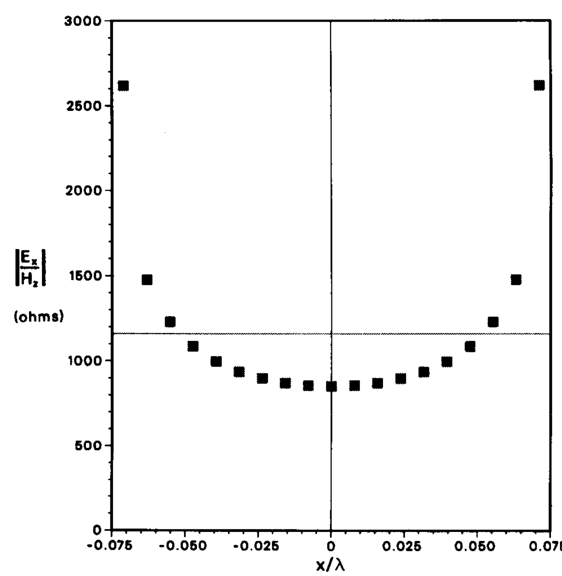

Fig. 6. Aperture impedance $|E_x/H_z|$ evaluated at $-w/2 < x < w/2$ and $y = 0$ for a rectangular gap with $\phi = \phi_0 = \pi/2$, $w/\lambda = 0.15$, and $d/\lambda = 0.2$: ■ exact, —— analytical.

of a finite element method [5] for H-polarization showed excellent agreement, and for purposes of comparison with the quasi-analytic solution, the moment method data will be regarded as exact.

Considering first the results for H-polarization, Fig. 3 shows the backscattering from a rectangular air-filled gap as a function of aspect for three gap widths. The aspect variation decreases with w. It is less than 4% for $w/\lambda = 0.15$, and since aspect independence is a feature of the quasi-analytic solution, we will henceforth confine attention to this case. It is then sufficient to take $\phi = \phi_0 = \pi/2$ corresponding to normal incidence backscatter.

In Figs. 4 and 5 the amplitude and phase of the far field amplitude $P_H(\pi/2, \pi/2)$ are shown as a function of depth for a rectangular air-filled gap of width $w/\lambda = 0.15$. We observe the cyclical behavior with zeros at $d/\lambda = 0, 0.5, 1.0, \cdots$, resulting from the periodicity of the impedance looking into the gap. From (39) and (21) the corresponding a are real and vary from $-\infty$ to ∞ over each cycle. Over the entire range of d/λ the agreement between the quasi-analytic and

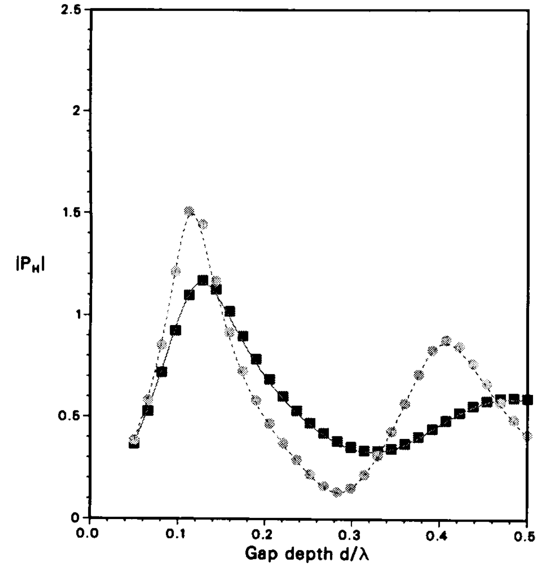

Fig. 7. Modulus of the far-field amplitude P_H for a material-filled rectangular gap of varying depth $d_1 = d$ with $\phi = \phi_0 = \pi/2$, $w/\lambda = 0.15$, and $\mu_r = 1$: $\epsilon_r = 2 + i1$ ■ exact, —— analytical; $\epsilon_r = 3 + i0.5$ ● exact, ------ analytical.

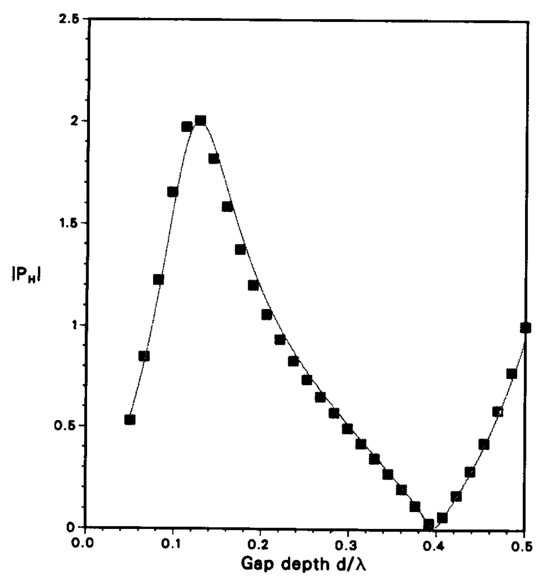

Fig. 8. Modulus of the far-field amplitude P_H for an air-filled L-shaped gap of varying depth $d_1 + d_2 = d$ with $\phi = \phi_0 = \pi/2$, $w/\lambda = 0.15$, $w_2/\lambda = 0.15$, and $d_1/d_2 = 3$: ■ exact, —— analytical.

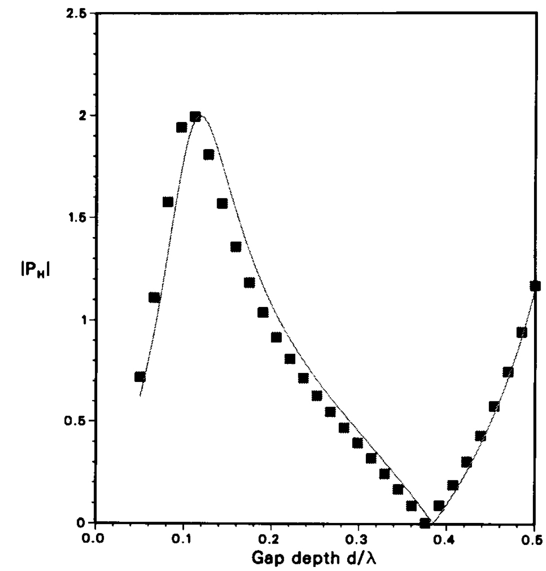

Fig. 9. Modulus of the far-field amplitude P_H for an air-filled T-shaped gap of varying depth $d_1 + d_2 = d$ with $\phi = \phi_0 = \pi/2$, $w/\lambda = 0.15$, $w_2/\lambda = w_3/\lambda = 0.075$, and $d_1/d_2 = 3$: ■ exact, —— analytical.

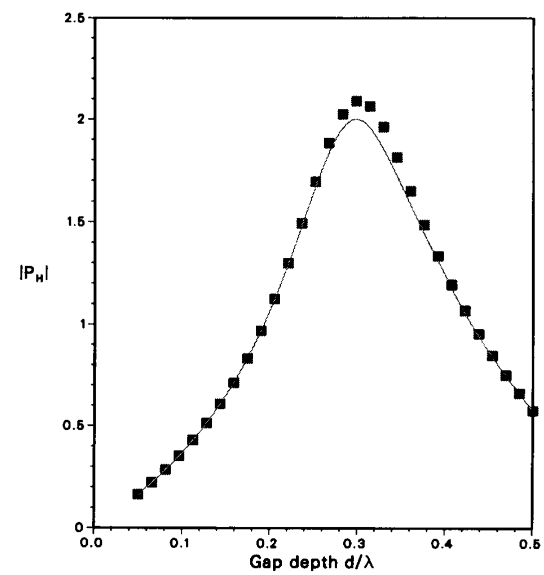

Fig. 10. Modulus of the far-field amplitude P_H for an air-filled V-shaped gap of varying depth $d_1 = d$ with $\phi = \phi_0 = \pi/2$ and $w/\lambda = 0.15$: ■ exact, —— analytical.

moment method results is excellent, but in spite of this the computed aperture impedances do not agree. This is evident from Fig. 6 where $|E_x/H_z|$ is plotted as a function of x for $w/\lambda = 0.15$ and $d/\lambda = 0.20$. The U-shaped behavior is in accordance with the edge condition at $x = \pm w/2$, and the data fit the curve $C\{1 - (2x/w)^2\}^{1/2}$ with $C = 860\ \Omega$. The average value is therefore $\pi C/2 = 1350\ \Omega$, compared with (36) which gives $|\eta| = 1160\ \Omega$. A similar discrepancy was found with all gap geometries. Nevertheless, the quasi-analytic solution provides an excellent approximation to the far field, and this is illustrated in Figs. 7–10 showing $|P_H|$ for a material-filled rectangular gap and for air-filled L-, T-, and V-shaped gaps.

Turning now to E-polarization, Fig. 11 shows the amplitude and phase of $P_E(\pi/2, \pi/2)$ as functions of w/λ for a rectangular air-filled gap having $d/\lambda = 0.1$. The quasi-analytic and exact data diverge with increasing w/λ, but the difference is less than 4% in amplitude and 5° in phase for $w/\lambda \leq 0.20$. For a rectangular gap with $w/\lambda = 0.15$, the quasi-analytic

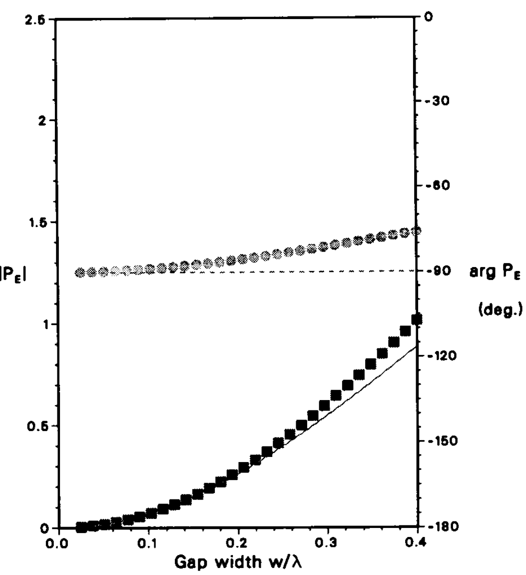

Fig. 11. Modulus and argument of the far-field amplitude P_E for an air-filled rectangular gap of varying width with $\phi = \phi_0 = \pi/2$ and $d/\lambda = 0.1$: modulus ■ exact, —— analytical, argument ● exact, - - - - - - analytical.

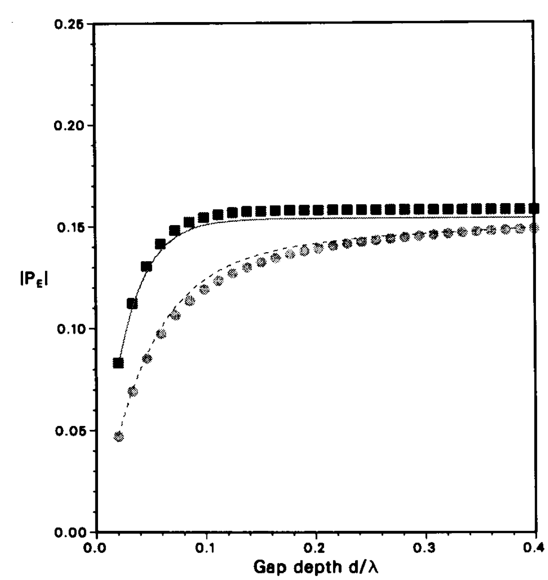

Fig. 12. Modulus of the far-field amplitude P_E for the air-filled rectangular and V-shaped gaps of varying depth $d_1 = d$ with $\phi = \phi_0 = \pi/2$ and $w/\lambda = 0.15$: rectangular ■ exact, —— analytical, V-shaped ● exact, - - - - - - analytical.

and exact results for $|P_E(\pi/2, \pi/2)|$ as a function of d/λ are presented in Fig. 12. The agreement is excellent, and as a consequence of the mode attenuation, the scattering is independent of the depth for $d/\lambda \geq 0.15$. A similar comparison for a triangular gap is also given in Fig. 12.

V. Conclusion

The quasi-analytic method described in [1] is based on the low frequency solution of the integral equations for a constant impedance insert in a perfectly conducting plane, and when used in conjunction with an estimate of the impedance looking into a gap, it provides a simple approximation to the far field scattering from the gap. To determine its accuracy, we have analyzed the problem of a plane wave incident on a gap backed by a cavity of arbitrary shape. The equivalence principle was used to develop coupled integral equations for the induced electric and magnetic currents, and the equations were then solved by the moment method. When the impedance looking into the cavity was determined using a transmission line model, it was found that for gap widths $w/\lambda \leq 0.15$ the quasi-analytic and moment method results for the scattered field were in excellent agreement for both polarizations and for all gap configurations tested. The same agreement is expected for arbitrary shaped gaps. It therefore appears that the quasi-analytic method is an efficient and effective tool for predicting the scattering from the junction where two component parts of a target come together.

Acknowledgment

The authors are grateful to Dr. R. A. Pearlman for his helpful comments.

References

[1] T. B. A. Senior and J. L. Volakis, "Scattering by gaps and cracks," *IEEE Trans. Antennas Propagat.*, vol. 37, pp. 744–750, June 1989.

[2] R. F. Harrington, *Time Harmonic Electromagnetic Fields.* New York: McGraw Hill, 1961, pp. 106 *et seq.*

[3] S. Ramo, J. R. Whinnery, and T. Van Duzer, *Fields and Waves in Communication Electronics.* New York: Wiley, 1984, p. 569.

[4] G. N. Watson, *A Treatise on the Theory of Bessel Functions.* Cambridge: Cambridge Univ. Press, 1948, p. 77.

[5] S. K. Jeng, "Aperture admittance matrix by finite element method for scattering by a cavity-backed aperture," presented at IEEE Antennas Propagat. Soc. Int. Symp., Syracuse, NY, June 1988.

Thomas B. A. Senior (SM'66–F'72) received the M.Sc. degree in applied mathematics from the University of Manchester, England, in 1950 and the Ph.D. degree in research from Cambridge University, Cambridge, England, in 1954.

In 1952 he was appointed an Established Scientific Officer and accepted a position with the Ministry of Supply at the Radar Research and Development Establishment (now the Royal Radar Establishment) at Malvern, England. In 1955 he was promoted to Senior Scientific Officer. He joined the Radiation Laboratory, University of Michigan, Ann Arbor, in June 1957. He was appointed Professor of Electrical Engineering and Computer Science in 1969. He served as Director of the Radiation Laboratory from 1975 to 1986, acting Department Chairman in 1987, and has been Associate Chairman of the Department since 1985. His primary interests are in the study of diffraction and propagation of electromagnetic waves, with applications to physical problems.

Dr. Senior has been an Associate Editor for *Radio Science* and served as Editor from 1973 through 1978, and is now an Associate Editor for *Electromagnetics.* He is Chairmen of Commission B of the International Union of Radio Science, the past Chairman of the U.S. National Committee for URSI and served as Chairman of the U.S. Commission B. He is a member of Sigma Xi, Tau Beta Pi, and Eta Kappa Nu, and is listed in *American Men and Women of Science.*

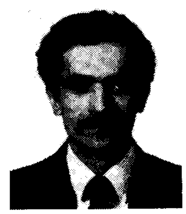

Kamal Sarabandi was born in Tehran, Iran, on November 4, 1956. He received the B.S. degree in electrical engineering from Sharif University of Technology, Tehran, Iran, in 1980, the M.S.E. degree in electrical engineering in 1986, the M.S. degree in mathematics, and the Ph.D. degree in electrical engineering in 1989, all from the University of Michigan, Ann Arbor.

From 1980 to 1984 he worked as a microwave engineer in the Telecommunication Research Center in Iran. He is currently an Assistant Research Scientist in the Department of Electrical Engineering and Computer Science at the University of Michigan. His research interests include electromagnetic scattering and microwave remote sensing.

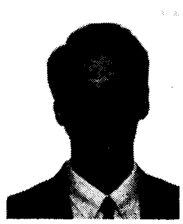

John R. Natzke (S'84) was born in Denison, IA, on August 28, 1963. He received the B.S.E.E. degree from Milwaukee School of Engineering, Milwaukee, WI, in 1985 and the M.S.E.E. degree from Marquette University, Milwaukee, WI, in 1988.

He has been pursuing the Ph.D. degree in electrical engineering at the University of Michigan, Ann Arbor, since September of 1988. His research interests include electromagnetic theory, scattering problems, and the numerical methods applied to these areas.

Mr. Natzke is a member of Eta Kappa Nu, and an associate member of Sigma Xi.